Maximization of Transmitted Acoustic Intensity from Silicon Integrated Piezoelectric Ultrasound Transducers

Wardhana, Gandhika K.; Mastrangeli, Massimo; Costa, Tiago L.

DOI
10.1109/IUS54386.2022.9957646

Publication date
2022

Document Version
Final published version

Published in
Proceedings of the IUS 2022 - IEEE International Ultrasonics Symposium

Maximization of Transmitted Acoustic Intensity from Silicon Integrated Piezoelectric Ultrasound Transducers

Gandhika K. Wardhana
Microelectronics Department
Delft University of Technology
Delft, the Netherlands
G.K.Wardhana@tudelft.nl

Massimo Mastrangeli
Microelectronics Department
Delft University of Technology
Delft, the Netherlands
M.Mastrangeli@tudelft.nl

Tiago L. Costa
Microelectronics Department
Delft University of Technology
Delft, the Netherlands
T.M.L.daCosta@tudelft.nl

***Abstract*—2D phased array ultrasonic transducers realized through the combination of bulk piezoelectric ceramics and complementary metal-oxide-semiconductor (CMOS) integrated circuits (IC) are enabling a new range of wearable ultrasound therapeutic applications. Traditional therapeutic ultrasound transducers have an air backing layer to maximize transmitted acoustic intensity. Yet, the pairing of piezoelectric transducers and silicon substrates commonly used in CMOS is still poorly understood. We integrated lead zirconate titanate (PZT) film on silicon membranes of various thicknesses to understand the impact of the silicon backing on the performance of bulk piezoelectric ultrasound transducers. The transducers with thinner silicon membranes exhibited higher acoustic intensity (up to 1.95 times while taking into account frequency shift), which is consistent with the simulation in finite element modeling. Transducers with silicon substrate also demonstrated a consistent shift to a higher resonance frequency.**

Keywords—piezoelectric ultrasound transducers, PZT integration, ultrasound neuromodulation

I. Introduction

Relevant and innovative biomedical applications of ultrasound such as neuromodulation [1] and power delivery to implantable devices [2],[3] require miniaturized ultrasound transducers with high transmitted acoustic intensity and high volumetric spatial resolution. The integration of 2D arrays of piezoelectric ultrasound transducers on complementary metal-oxide-semiconductor (CMOS) integrated circuits (IC)[4] can meet at once the demand for transducer miniaturization, steerable focal point, and high-volumetric spatial resolution via 3D ultrasound transmit beamforming [5]. However, current implementations of 2D phased arrays in CMOS are still limited in output intensity range, in particular when compared to commercial single-element transducers used in ultrasound neuromodulation [1], [6]. Adoption of CMOS IC to drive the transducer implies using acoustic backing layers mainly composed of the silicon substrate, which, opposing to the commonly used air backing layer [7], is not optimized for maximizing acoustic transmission efficiency Fig. 1. Improving the transmission efficiency of piezoelectric transducers on silicon substrate would greatly benefit ultrasound applications with limited power supply (e.g., portable and wearable devices).

This study proposes a fabrication method to integrate an air-cavity and mitigate the effect of silicon as the backing layer of piezoelectric transducers on the generated acoustic intensity. The air-cavity is introduced by controllably thinning down the silicon substrate in correspondence with the transducer to observe the effect of different thicknesses of silicon on the acoustic intensity. The work is organized as follows: Section II discusses the simulation, fabrication process, and experimental setup used in this study. Section III presents the simulation and experimental results. Section IV concludes the paper.

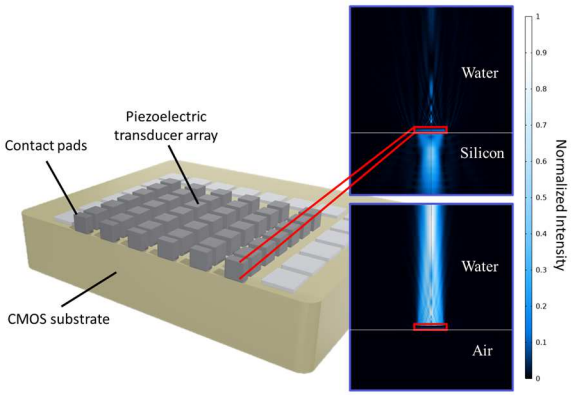

Fig. 1. Sketch of a 2D phased array on CMOS chip with simulated normalized ultrasound intensity with 300 µm-thick silicon backing and with air-backing.

II. Methods

A. Simulation

We used COMSOL Multiphysics to simulate the impact of silicon substrate thickness on acoustic intensity generated by a piezoelectric ultrasound transducer. In this study, a 2D axisymmetric geometry was chosen to significantly reduce the computational time of the simulation. Fig. 2 shows the ultrasound transducer model used in COMSOL. The transducer consists of a lead zirconate titanate (PZT) die in contact with a 300 µm-thick silicon chip. The PZT is aligned with a supporting silicon membrane with varying thicknesses.

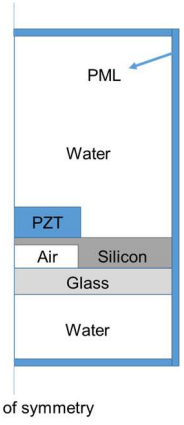

Fig. 2. Sketch of COMSOL axisymmetric simulation model.

2022 IEEE International Ultrasonics Symposium (IUS) | 978-1-6654-6657-8/22/$31.00 ©2022 IEEE | DOI: 10.1109/IUS54386.2022.9957646

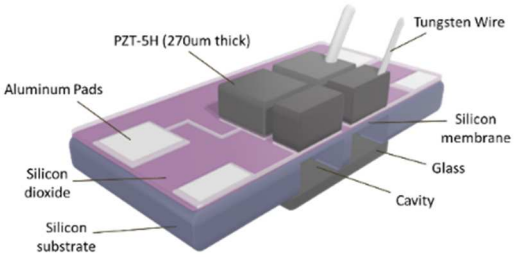

Fig. 3. Model of the fabricated piezoelectric transducer with air-backing layer.

A layer of glass is placed underneath to seal the air cavity. Water is chosen as the propagation medium of the acoustic waves, as it acoustically mimics soft tissue. A perfectly matched layer (PML) enclosed the boundary of the medium to avoid acoustic reflections.

B. Device Fabrication

Based on the simulation, a prototype of the transducer was fabricated on a 4-inch Si wafer. The design of the device can be seen in Fig. 3.The process started with a 300-µm-thick P-type silicon wafer. Then, 400 nm of silicon dioxide was deposited using plasma-enhanced chemical vapor deposition (PECVD). A layer of 400-nm Aluminum with 1% silicon was sputtered on top of the silicon dioxide. The aluminum layer was patterned using photolithography and reactive ion etching (RIE) to create interconnects. Another layer of PECVD silicon dioxide (400 nm-thick) was deposited to encapsulate the aluminum layer. Contact openings were made by using a wet etching process with buffered hydrofluoric acid (BHF 7:1). A 8-µm-thick layer of photoresist (AZ-12XT-20PL-10, MicroChemicals) was later spin-coated on the back of the wafer as a masking layer. The silicon layer underneath transducer pads in the array was removed using deep reactive ion etching (DRIE), leaving only a membrane of silicon dioxide (completely removed silicon), 20-µm-thick silicon, and 50-µm-thick silicon, respectively, supporting the aluminum layer. Afterward, the wafer was diced into individual square dies with the size of 33 x 33 mm^2. Subsequently, the backside of the array was covered by glass cover plates and sealed on the edge using epoxy (EPO-TEK 301-2FL, Epoxy Technology). In this process, 2.8 x 2.8 mm^2 chips diced from pre-polled 267-µm-thick PZT-5H (piezo.com) were mounted on the membranes and electrically connected by using silver-filled epoxy (EPO-TEK H20E, Epoxy Technology). Tungsten wire with a diameter of 50 µm was attached to the PZT as a ground terminal using silver-filled epoxy. Finally, the entire device was encapsulated with 5-µm-thick CVD Parylene-C.

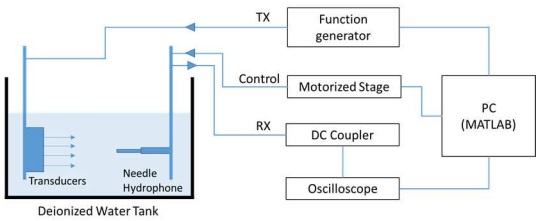

Fig. 4. Diagram of the measurement setup

C. Measurement Setup

The characterization of the transducer was performed using the setup sketched in Fig. 4 and the protocol hereby described. The fabricated transducer was placed in a tank filled with deionized water using a 3D-printed holder (Fig. 5). A pre-calibrated (~ 1.35 µV/Pa) 1-mm diameter needle hydrophone (NH1000, Precision Acoustics) connected its respective preamplifier and an oscilloscope (DSO-X 3032A, Agilent Technologies) was used to characterize the generated ultrasound pressure. The hydrophone and its preamplifier are mounted on a 3-axis motorized stage (VK-62000, GAMPT mbH) controlled by a stage controller (SFS630, GAMPT mbH). The signal to drive the transducer was provided by a function generator (DG4202, RIGOL). The oscilloscope, function generator, and stage controller were connected to a computer with a graphical user interface to control all the components during the measurement. The transducer was driven with bursts of a 10 Vpp-square wave with a fundamental frequency of 8 to 10 MHz, pulse repetition frequency (PRF) of 1 kHz, and each burst containing 40 waves. The number of waves in a burst was chosen to be long enough to ensure the burst reached its peak intensity while not introducing any electromagnetic interference in the hydrophone during the ultrasound measurement. The hydrophone was placed 10 mm away from the fabricated device. The distance was calculated by using the propagation time and the speed of sound in water.

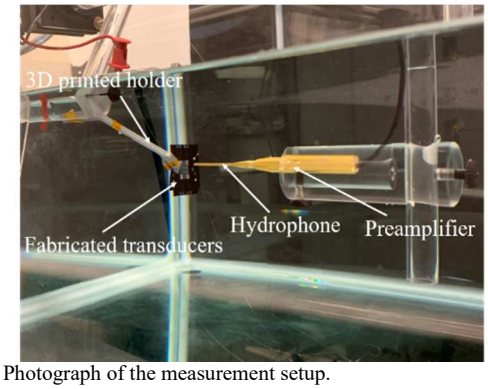

Fig. 5. Photograph of the measurement setup.

III. Results and Discussion

Based on the simulation result (Fig. 6), the generated intensity generally becomes lower with respect to the increasing thickness of the silicon underneath, though the trend is not monotonic. There are four points of interest which is where

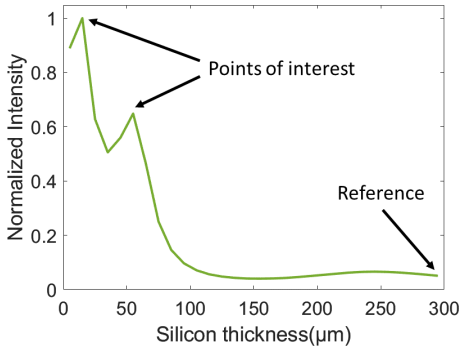

Fig. 6. The effect of membrane thickness to the generated (normalized) intensity of transducers at 8 MHz center frequency simulated in COMSOL

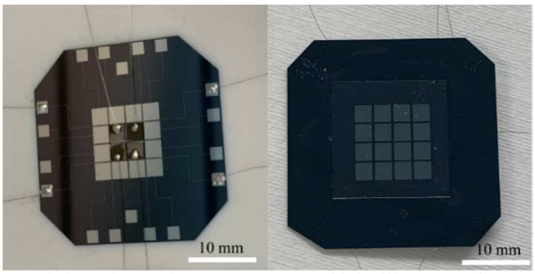

Fig. 7. Fabricated transducer on a 20-µm-thick silicon membrane, front-view (left) and back-view (right).

the silicon is completely removed, 20-µm-thick silicon, 50-µm-thick silicon, and a reference wafer with an intact 300-µm-thick silicon layer on the back of the piezoelectric layer. In respect to these points of interest, four sets of transducers were fabricated following the procedure described in Section II.B. One of the transducers is shown in Fig. 7.

Fig. 8(a) shows the readout of the hydrophone in a single measurement. Since changing the ultrasound frequency leads to a change in natural focal spot depth, the peak-to-peak intensity for each sample was recorded along the propagation direction while sweeping the ultrasound frequency. The results obtained for the transducer with the extreme cases of the backing layer are shown in Fig. 8(b) and Fig. 8(c), for a 20-

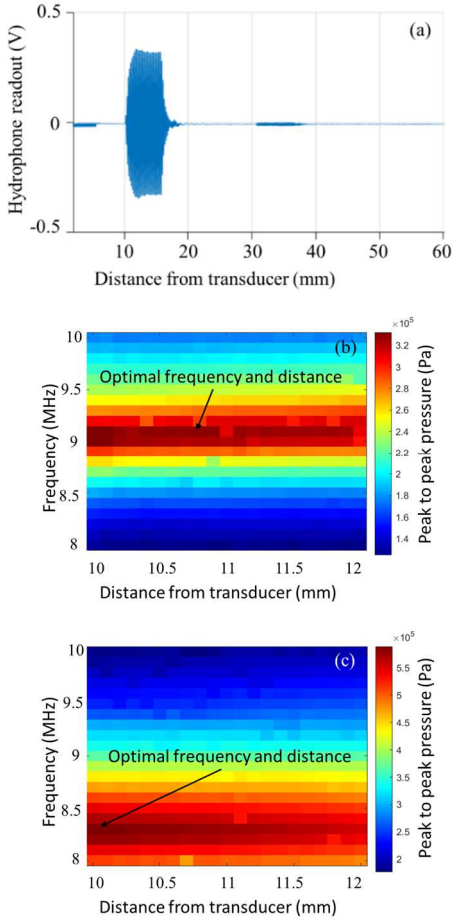

Fig. 8. An example of a single readout from the hydrophone (a). The distance and frequency sweep of a transducer with 20-µm membrane backing layer (b) and a reference transducer (c).

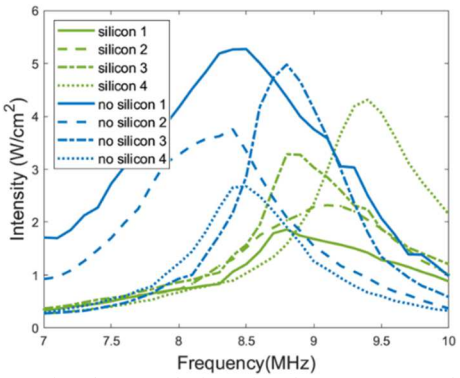

Fig. 9. Comparison between the intensity of two groups transducers with an intact silicon substrate (4 transducers) and completely removed silicon membrane (4 transducers).

µm silicon membrane and the 300 µm-thick reference silicon substrate, respectively.

From the measurements shown in Fig. 8 for all samples, the natural focal depth for every frequency was determined. With this information, the acoustic intensity for four transducers with silicon completely removed and four transducers with the reference 300 µm-thick silicon backing substrate were measured, with the hydrophone positioned at the distance corresponding to the peak intensity. The results are shown in Fig. 9. Despite some dispersion in the results, there is a clear increase in intensity by completely removing the silicon backing. To investigate this further, the intensity of all test samples was measured, in the same conditions, with the results shown in Fig. 10. Both Fig. 9 and Fig. 10 show that the implementation of the air backing layer improves the intensity of ultrasound in correspondence to the respective resonance frequencies when compared to the reference, and that this improvement increases with the decreased thickness of silicon-backing. Along with the improvement in intensity, we observed a consistent decrease in resonance frequency when compared to the reference. When considering the thickness of the piezoelectric sheet, a resonance frequency of ~8.5 MHz is expected. From Fig. 9, the average resonance frequency of the reference group was 9.025 MHz, while in the group with silicon completely removed, it was 8.55 MHz. This indicates that the presence of silicon as a backing layer shifts the resonance frequency of the PZT transducer upward.

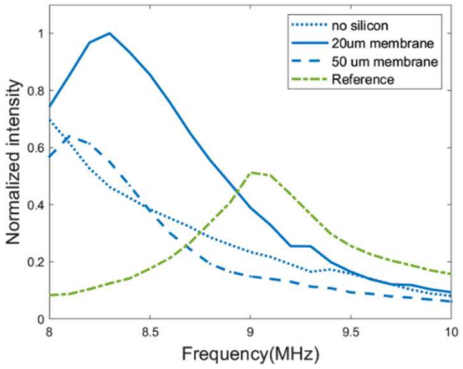

Fig. 10. Normalized intensity of test samples with the center frequency of 8 to 10 MHz

Furthermore, it also emphasizes the importance of the backing layer and its influence on the resonance frequency

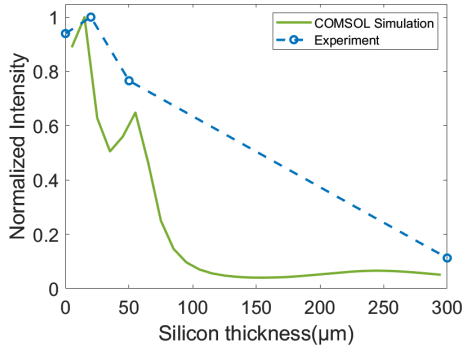

Fig. 11. Comparison between simulation and experimental results at fixed 8MHz center frequency.

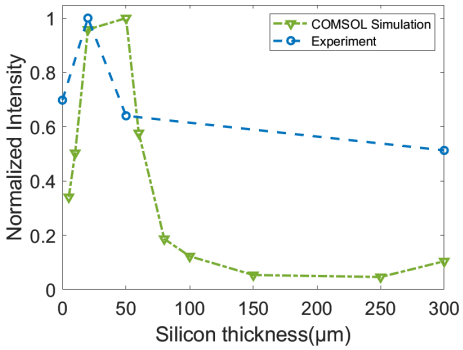

Fig. 12. Comparison between simulation and experimental results adjusting to the change of resonance frequency.

when designing the driving circuitry to 2D arrays of ultrasound transducers.

In Fig. 11, the simulations and experimental results were compared at 8 MHz center frequency. It shows that the experimental result follows a similar trend to the simulation result when comparing the point of interests.

In Fig. 12, compensation was performed for the shift in resonance frequency in both simulation and experiment. A frequency sweep was performed on each membrane thickness. Then the maximum intensity was taken at the resonance frequency of each sample. Similar behavior is seen in both Fig. 11 and Fig. 12, with a drop in intensity at membrane thickness below 20 µm. The increase in intensity from the reference in Fig. 11 (up to 8.89 times) is significant, though less stark when compared to the result in Fig. 12, with the intensity adjusted to take into account the resonance frequency change (up to 1.95 times).

Another critical observation concerns the consistent increase of the intensity of transducers on 20 um-thick and 50 um-thick membranes when compared to the reference throughout the experiments and simulations. This makes this technique promising to implement in a CMOS substrate, which has been demonstrated in other CMOS devices thinned down to 20-µm without affecting their performance [8], [9].

IV. Conclusion

We presented a study on the impact of the silicon substrate on the performance of bulk piezoelectric ultrasound transducers. We proposed the implementation of an air backing layer to maximize the transmitted acoustic intensity through the etching process of the silicon substrate in a wafer-scale process. We compared groups of ultrasound transducers with different membrane thicknesses and showed that transducers backed by thinner silicon membranes generate higher acoustic intensity when compared to the reference. A shift to a higher resonance frequency was constantly observed on bulk ultrasonic transducers with silicon backing. As the frequency is a crucial parameter in designing a pitch-matched phased array transducer [5], the evidenced frequency shift should inform the design of the transducer and driving electronics. The results presented in this study also encourage further investigation of the effect of implementing an air backing layer on a CMOS substrate.

References

[1] J. Blackmore, S. Shrivastava, J. Sallet, C. R. Butler, and R. O. Cleveland, "Ultrasound Neuromodulation: A Review of Results, Mechanisms and Safety," *Ultrasound in Medicine and Biology*, vol. 45, no. 7. 2019. doi: 10.1016/j.ultrasmedbio.2018.12.015.

[2] G. Luca Barbruni, P. Motto Ros, D. Demarchi, S. Member, S. Carrara, and D. Ghezzi, "Miniaturised Wireless Power Transfer Systems for Neurostimulation: A Review," *IEEE Trans Biomed Circuits Syst*, vol. 14, no. 6, 2020, doi: 10.1109/TBCAS.2020.3038599.

[3] C. Shi, T. Costa, J. Elloian, Y. Zhang, and K. L. Shepard, "A 0.065-mm^3 Monolithically-Integrated Ultrasonic Wireless Sensing Mote for Real-Time Physiological Temperature Monitoring; A 0.065-mm^3 Monolithically-Integrated Ultrasonic Wireless Sensing Mote for Real-Time Physiological Temperature Monitoring," *IEEE Trans Biomed Circuits Syst*, vol. 14, no. 3, 2020, doi: 10.1109/TBCAS.2020.2971066.

[4] C. Shi, T. Costa, J. Elloian, and K. L. Shepard, "Monolithic Integration of Micron-scale Piezoelectric Materials with CMOS for Biomedical Applications," *Technical Digest - International Electron Devices Meeting, IEDM*, vol. 2018-December, pp. 4.5.1-4.5.4, Jan. 2019, doi: 10.1109/IEDM.2018.8614632.

[5] T. Costa, C. Shi, K. Tien, J. Elloian, F. A. Cardoso, and K. L. Shepard, "An Integrated 2D Ultrasound Phased Array Transmitter in CMOS With Pixel Pitch-Matched Beamforming; An Integrated 2D Ultrasound Phased Array Transmitter in CMOS With Pixel Pitch-Matched Beamforming," *IEEE Trans Biomed Circuits Syst*, vol. 15, no. 4, 2021, doi: 10.1109/TBCAS.2021.3096722.

[6] A. Fomenko, C. Neudorfer, R. F. Dallapiazza, S. K. Kalia, and A. M. Lozano, "Low-intensity ultrasound neuromodulation: An overview of mechanisms and emerging human applications," *Brain Stimul*, vol. 11, no. 6, pp. 1209–1217, Nov. 2018, doi: 10.1016/J.BRS.2018.08.013.

[7] H. S. Gougheri, A. Dangi, S. R. Kothapalli, and M. Kiani, "A Comprehensive Study of Ultrasound Transducer Characteristics in Microscopic Ultrasound Neuromodulation," *IEEE Trans Biomed Circuits Syst*, vol. 13, no. 5, pp. 835–847, Oct. 2019, doi: 10.1109/TBCAS.2019.2922027.

[8] S. Moazeni et al., "19.2 A Mechanically Flexible Implantable Neural Interface for Computational Imaging and Optogenetic Stimulation over 5.4×5.4 mm 2 FoV," *2021 IEEE International Solid-State Circuits Conference (ISSCC)*, 2021, pp. 288-290, doi: 10.1109/ISSCC42613.2021.9365796.

[9] S. Zucca *et al.*, "Effects of Substrate Thinning on the Properties of Quadruple Well CMOS MAPS," in *IEEE Transactions on Nuclear Science*, vol. 61, no. 2, pp. 1039-1046, April 2014, doi: 10.1109/TNS.2014.2307960.